MATHEMATICAL MODELLING AND PERFORMANCE EVALUATION OF THE CM14 TURBOJET ENGINE

Farah H. Al-Amari, Marwa A. Kaeber and Saleh Basha Alkhodari

Faculty of Engineering, Aeronautical Department, University of Tripoli, Libya
Email: f.lamari@aerodept.edu.ly

الملخص

يركز هذا العمل على إيجاد وتحليل معاملات الأداء للمحرك النفاث النموذجي المعملي CM14، من خلال إيجاد وتحليل متغيرات الأداء للمحرك. تم تكوين نموذج رياضي متكامل للمحرك النفاث CM14 عن طريق إيجاد معادلات رياضية تفصيلية لكل مكوّن من مكونات المحرك المختلفة. النموذج المشتق سوف يساعد في دراسة أداء المحرك عند ظروف تشغيل مختلفة من غير اللجوء إلى إجراء تجارب عملية قد تكون مكلّفة من ناحية الثمن والوقت. تمت محاكاة النموذج المشتق باستعمال MATLAB وSimulink. وللتأكد من أن النموذج المشتق يمكن الاعتماد عليه في دراسة أداء المحرك ومعرفة مدى دقته، تمت مقارنة النتائج التي تم الحصول عليها من هذا النموذج مع النتائج العملية المتحصل عليها من المحرك النفاث CM14 الحقيقي عند تشغيله عند أقصى دورة له في الدقيقة وباستخدام نفس المدخلات. المقارنة أظهرت أن نتائج النموذج المشتق تعتبر معقولة ومرضية.

ABSTRACT

This work focuses on evaluating the performance of a laboratory model CM14 turbojet engine through finding and analyzing the engine performance parameters. An integrated mathematical model was developed for the CM14 turbojet engine by deriving the detailed equations for the different engine components. The derived engine model will help in studying the engine performance at different operating conditions without performing heavily expensive experiments. Simulations for the derived model were carried out using MATLAB and Simulink. To ensure the reliability of the derived model the obtained results from the simulation were compared with an experimental data from the real CM14 turbojet engine at maximum rpm. The comparison shows that the obtained performance parameters from the derived model are reasonable and satisfactory.

KEYWORDS: Mathematical Modelling; Simulation; Performance; CM14 Turbojet Engine.

INTRODUCTION

Aircraft engine represents the heart of an aircraft exactly as the heart of a human being. The turbojet is an airbreathing jet engine, typically used in aircraft; it consists of a gas turbine with a propelling nozzle [1]. The CM14 Turbojet engine, shown in Figure (1), is a complete aeronautical axial flow gas turbine engine. The engine itself is a small compact Olympus HP E-start turbine engine, comprising a single stage radial compressor, annular combustion chamber, and a low mass, high performance axial flow turbine [2]. Full instrumentation is included as standard, allowing the measurement of a wide range of variables such as temperature, pressure, air, and fuel flows, thrust and shaft speed. Studying the viability and performance of the jet engine through calculating its performance parameters. Deriving the mathematical model for the engine by developing the detailed equations for the different components of the engine will help in developing the performance parameters. Some of Previous studies are Zare, Fo. et. al. [3], a concentrated parameter distribution type mathematical model has been developed and implemented in MATLAB environment for modelling thermodynamically cycles and characteristics of the single spool no bypass jet engines. The results of the analysis are compared with available operational data of the Tumansky R-29 type turbojet engine at sea level static condition, the simulation results show less than or equal 10.2 percent difference between the simulated and the available real data. Ujam, A. et. al. [4] presented an approach to analyze the performance of jet engine with an alternative flow control mechanism by regulating the flow at the engine inlet to increase the engine rpm for the same value. The work focused on performance characteristics of turbojet with reduced inlet pressure to the compressor engine. Simulink was used for dynamic modelling of the engine. Performance parameters of the engine are analyzed with the increase in compressor pressure ratio and shaft rpm. Tudosie, A. N., [5] presented a single-spool jet engine's rotation speed's control system, which has integrated a fuel flow rate injection controller meant to insure the speed and the temperature limitation during the engine's transient operating regimes. An improvement has been realized for a previously presented mathematical model for the system. Tudosie, A. N.,[6] deals with a fuel system meant to assure the fuel supply of an aircraft turbo-jet engine's afterburner, with respect to the aircraft's flight regime. The non-linear motion equations were established for the integrated system (afterburning fuel pump-flight regime corrector); based on it, assuming the small perturbations hypothesis, these equations were transformed into a linear system. All output parameters are stabilizing at their new values with static errors, so the system is a static system; however, the static errors are acceptable. Tudosie, et. al. [7] deals with a single-spool single jet engine with afterburner for thrust augmentation. The authors have studied engine-afterburning system time behavior, by studying its quality, which means its time response. To keep the gas-turbine pressure ratio constant, the engine's fuel flow rate and nozzle exhaust opening must be controlled. The simulations were based on some coefficient, experimentally determined, and calculated for the VK-1F jet engine. Abeykoon, C. [8] implemented a pre-established equation in MATLAB and Simulink to create a model for a turbojet engine. The influence of atmospheric conditions was considered in creating the model. The theoretical and Simulink models were in a good agreement within reasonable limits, which verifies the correctness of the Simulink model established in this work. Ishola A. Afiz et. al. [9] aimed to control an aircraft fuel system by means of adopting control systems engineering principles and methods to understand the applications of control systems in managing an aircraft fuel system. A mathematical model was developed for the fuel system and simulated using MATLAB-Simulink software to analyze the fuel consumption rate. The system was tuned with a Proportional Integral and Derivative (PID) controller. The obtained results were validated with similar analogous. Ryszard Chachurski et. al. [10], their objective was to calculate the performance of gas-dynamic of a GTM 120 miniature turbojet engine by determining the performance parameters and compare it with the theory contained in the literature and laboratory results. Their obtained results in the analytical method are very similar to those obtained in the computer calculations and both methods are deviated with a similar level from the real results. Richa Singh et. al. [11] developed a mathematical model for the SR-30 laboratory gas turbine engine to obtain a shaft speed response with a fuel flow as input. To develop the model, they have been used approximated maps and governing equations that describe the engine behavior. Then the obtained results compared with an experimental data. The comparison showed good results with small differences in results for both steady state and transient conditions. The derived model is tuned with a designed PID controller. Velásquez-SanMartín et. al. [12] proposed a mathematical model for the fuel consumption analysis during aircraft cruise. A closed-form formula for the aircraft's weight as a function of time during the cruising flight phase is presented. To obtain such formula, the equations of motion for this flight phase are considered along with the fuel consumption relationship. The obtained formula is a closed-form solution of a certain differential equation. The model results are very close to the reality. This paper focuses on deriving a mathematical model for the CM14 turbojet engine, then evaluating the engine performance parameters by simulating the derived model using MATLAB and Simulink. Then the simulated results will be compared with a real engine data at a certain operating point using the same input data to the two models for calculating the engine performance parameters.

Figure 1: CM14 Turbojet engine [2].

ENGINE MODELING

A mathematical model will be derived for the CM14 turbojet engine with basic components, inlet, compressor, combustor, turbine, and nozzle. The derived model will help in studying the engine performance at different operating conditions without performing heavily expensive experiments. All operational gas processes in a jet engine are irreversible due to friction. Thus, the compressor, turbine and nozzle isentropic efficiencies will be assumed and applied beside the pressure loss in the intake and combustion chamber. The burning efficiency will also be considered. With respect to Figure (2), the flow enters gas turbine over section (a-2). The air is compressed and delivered from section 2 to section 3 by the compressor, while the combustion process occurs between sections 3 and 4. The turbine is located between sections 4 and 5. The final part of the engine is the exhaust nozzle, which is located between sections 5 and 9.

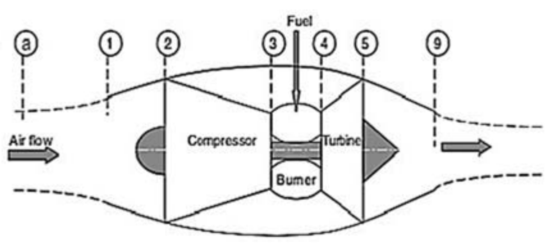

Figure 2: Station numbering for the engine modelling [13].

Mathematical Model

Steady thermo-dynamical equations are used for calculating and plotting the real cycle of the engine process in T-s diagram [14]. Only some of the mathematical equations that were used in describing the engine are listed here.

Ambient properties

The stagnation ambient air temperature and pressure can be calculated for the given flight Mach number from the following equations

$$T_{o1} = T_a\left(1 + \frac{\gamma_c - 1}{2} M_a^2\right) \qquad (1)$$

$$P_{o1} = P_a\left(1 + \frac{\gamma_c - 1}{2} M_a^2\right)^{\frac{\gamma_c}{\gamma_c - 1}} \quad (2)$$

Inlet

The inlet performance is defined by the pressure recovery from the free stream to the engine. The process in the intake can be achieved by the constant total temperature and determining the total pressure by the pressure recovery factor of the intake as:

$$T_{o2} = T_{o1} \quad (3)$$

$$P_{o2} = r_d\, P_{o1} \quad (4)$$

However, the diffuser efficiency η_d can be expressed and calculated from the following equation:

$$P_{o2} = P_1\left(1 + \eta_d \frac{(\gamma_c - 1)}{2} M_1^2\right)^{\frac{\gamma_c}{\gamma_c - 1}} \quad (5)$$

Compressor

The outlet total pressure of the compressor is calculated by the knowledge of the total pressure ratio of the compressor and the intake outlet total pressure:

$$P_{o3} = r_c P_{o2} \quad (6)$$

The total temperature from the compressor outlet can be calculated by knowing the isentropic efficiency, η_c , equation (8).

$$T_{o3s} = T_{o2}\left(\frac{p_{o3}}{p_{o2}}\right)^{\frac{\gamma_c - 1}{\gamma_c}} \quad (7)$$

$$T_{o3} = \frac{T_{o3s} - T_{o2}}{\eta_c} + T_{o2} \quad (8)$$

Combustion chamber

The stagnation pressure at the outlet of combustion chamber, state (4), is less than its value at the inlet because of the real flow assumption. Thus, the outlet pressure of the combustion chamber is expressed as follows:

$$P_{o4} = r_{cc}\, P_{o3} \quad (9)$$

The fuel to air ratio is calculated by taking into consideration the burner efficiency, η_b, equation (10) in the function of combustion chamber and turbine inlet total temperature.

$$f = \frac{Cp_m \times (T_{03} - T_{04})}{(1 + L_o)\left(Cp_{T_{o4}} \times T_{o4}\right) - \left(L_o \times Cp_{T_{o4}}\right) - (Q_R \times \eta_b)} \quad (10)$$

The $C_{p_{T04}}$ is the real specific heat of the air at turbine inlet total temperature at constant pressure. The mass flow rate of the fuel comes from

$$\dot{m}_f = f\, \dot{m}_a \quad (11)$$

Turbine

By using the energy balance of the spool, the turbine exit temperature is obtained as follows

$$T_{o5} = T_{o4} - \frac{C_{p_c} \times (T_{o3} - T_{o2})}{(1 + f) C_{p_{T_{o4}}} \times \eta_m \times \zeta} \quad (12)$$

The turbine outlet isentropic total temperature can be determined by.

$$T_{o5s} = T_{o4} - \frac{T_{o4} - T_{o5}}{\eta_T} \quad (13)$$

The outlet total pressure of the turbine is calculated by

$$P_{o5} = \left(\frac{P_{o4}}{\left(\frac{T_{o4}}{T_{o5s}} \right)} \right)^{\frac{\gamma_h}{\gamma_h - 1}} \quad (14)$$

Nozzle

The exit velocity from the convergent is given by

$$V_9 = \sqrt{2 \times C_{p_{To4}} \times \eta_n \times T_{o5} \left(1 - \left(\frac{P_a}{P_{o5}} \right) \right)^{\frac{\gamma_h - 1}{\gamma_h}}} \quad (15)$$

In equation (17), the nozzle outlet static temperature is determined by the available nozzle efficiency, η_n, and isentropic static temperature of the nozzle T_{9s}, which comes from equation (16).

$$T_{9s} = T_{o5} \left(\frac{P_a}{P_{o5}} \right)^{\frac{\gamma_h - 1}{\gamma_h}} \quad (16)$$

$$T_9 = T_{o5} - \eta_n (T_{o6} - T_{9s}) \quad (17)$$

Engine Performance Parameters

The performance of an aircraft engine may be rated by its ability to provide the necessary thrust force in propelling an aircraft efficiently. The engine performance parameters are identified as:

Thrust

The thrust force can be expressed as following:

$$\tau = \dot{m}_a \big((1 + f) V_9 - V_a \big) + A_9 (P_9 - P_a) \quad (18)$$

A_9 is the nozzle outlet area.

Thrust specific fuel consumption (TSFC)

Changing the mass flow rate of air influences the specific fuel consumption (SFC) and the thrust. The TSFC is given by the following equation:

$$TSFC = \frac{\dot{m}_f}{\tau} \quad (19)$$

Thermal efficiency

The engine thermal efficiency is defined as the rate of addition of kinetic energy to the air divided by the rate of fuel energy supplied.

$$\eta_{th} = \frac{\tau V_a + \frac{1}{2} \dot{m}_a (1 + f)(V_9 - V_a)}{\eta_b \, \dot{m}_f \, Q_R} \quad (20)$$

Propulsive and burning efficiency

The propulsive efficiency is the ratio of the useful propulsive power produced by the engine to the rate of kinetic energy addition to the air, equation (21).

$$\eta_p = \frac{\tau V_a}{\tau V_a + 0.5\dot{m}_a(1+f)(V_9 - V_a)^2} \quad (21)$$

The burning efficiency is denoted, η_b, can be considered from

$$\eta_b = \frac{(\dot{m}_f Q_R)_{actual}}{(\dot{m}_f Q_R)_{ideal}} \quad (22)$$

Overall efficiency

The overall efficiency which is the ratio of useful power and the energy supplied by the fuel can be calculated from the product of the propulsive, thermal and the burning efficiencies.

$$\eta_o = \eta_b \, \eta_{th} \, \eta_p \quad (23)$$

or

$$\eta_o = \frac{\tau V_a}{\dot{m}_f Q_R} \quad (24)$$

Thermodynamic cycle

The T-s diagram of the ideal Brayton cycle is shown in Figure (3), the cycle processes are explained in Table (1).

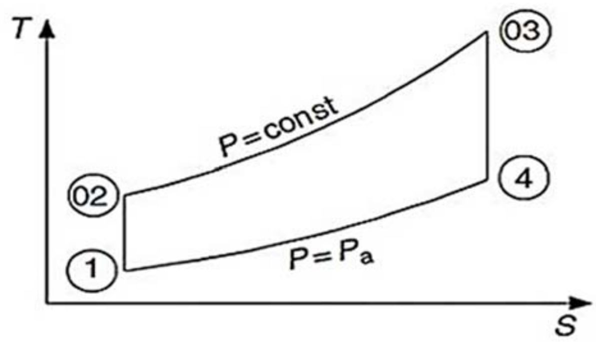

Figure 3: T-s Diagram for the ideal closed Brayton cycle [1].

Table 1: Ideal closed Brayton cycle processes.

1-2	Isentropic compression
2-3	Constant pressure heat addition
3-4	Isentropic expansion
4-1	Constant pressure heat rejection.

Ideal cycle for turbojet engine

T-s diagram of the ideal jet engine cycle is shown in Figure (4). The air pressure increases slightly in the diffuser as its speed is decelerated. It is compressed in the compressor to the highest pressure in the cycle. Then, it is mixed with the fuel in the combustion chamber, where the mixture is burned at constant pressure. The high pressure and temperature combustion gases partially expand in the turbine, producing enough power to drive the compressor and the other auxiliary equipment. Finally, the gases expand to the ambient pressure through the nozzle and leave at a high velocity [14].

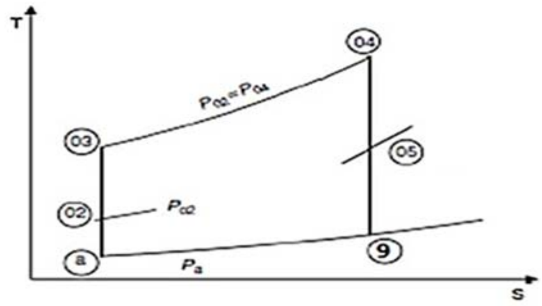

Figure 4: T-s diagram of the ideal turbojet cycle [1].

Table 2: Ideal turbojet cycle processes

a-2	Isentropic decelerates in diffuser
2-3	Isentropic compression
3-4	Constant pressure heat addition
4-5	Isentropic expansion through turbine
5-9	Isentropic expansion across an exhaust nozzle

MODEL SIMULATION

To study the engine performance parameters, the derived engine model was simulated using MATLAB and Simulink techniques. The obtained results from the simulated model were compared with experimental results from the real CM14 turbojet engine that carried out at the laboratory.

Components Model Simulation

The engine model using the non-linear component dynamics in a continuous time sample is developed in Simulink workspace by using the derived model. The input values are the material properties of the operational fluids, geometrical engine data, flight speed, compressor total pressure ratio, total inlet turbine temperature and air mass flow rate, and the assumed efficiencies of the different components of the jet engine model. Some of these inputs are not available, for example the component efficiencies. So, it is approximated from the values listed in [3].

Table 3: Input data

Environmental conditions and reference values		Material Properties and constants		Power reduction coefficients	
S_o [J/kg. K]	1000	M_a [kg/k mol]	28.97	η_n	0.952
P_a [Pa]	101325	**Lo**	42.17	η_T	0.866
T_a [K]	293.15	γ_a	1.4	η_C	0.971
V_o [m/s]	102.04	γ_g	1.33	η_b	0.93
H [m]	0	R_a [J/kg. K]	288.5714	η_m	0.91
Geometry and operational data of the engine		R_g [J/kg. K]	282.8	r_{cc}	0.93
r_c	2.1	Q_r [MJ/kg]	42.80	ζ	0.92
T_{o4} [K]	802.15	R_m [J/k mol. K]	8314	r_d	0.94
$\dot{m}_a$ [kg/s]	0.59	$C_{p\ com}$ [J/kg. K]	1010		
d_1 [m]	0.0732	$C_{p\ m}$ [J /kg. k]	1090		
d_9[m]	0.0859	$C_{p\ To4}$ [J/kg. k]	1100		

The different engine components are represented in Simulink as below.

Ambient and inlet models

Ambient atmospheric and inlet properties are modelled in Simulink as shown in the Figures (5) and (6) respectively. Where the given input to the model is the altitude and the output will be the total values of the temperature and pressure, which are available for the engine inlet.

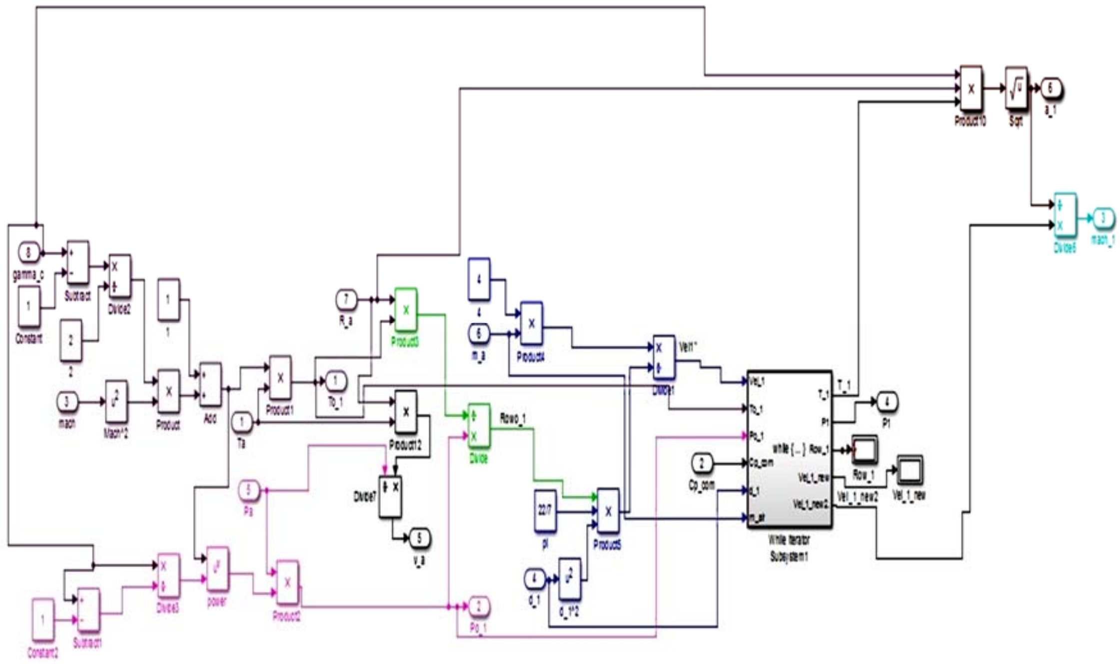

Figure 5: Ambient properties model.

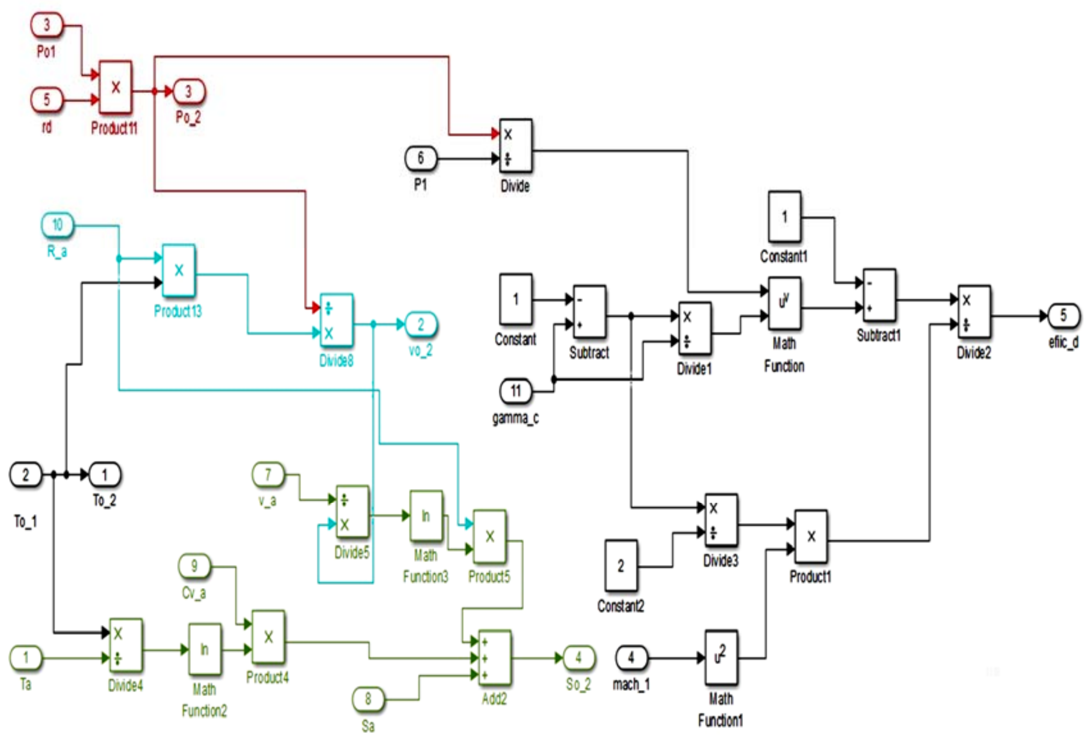

Figure 6: Inlet model.

Compressor model

The compressor is represented in Simulink as shown in Figure (7). The computed variables are the compressor exit pressure, entropy, temperature, and specific volume. All the other engine components are represented in the Simulink by the same way.

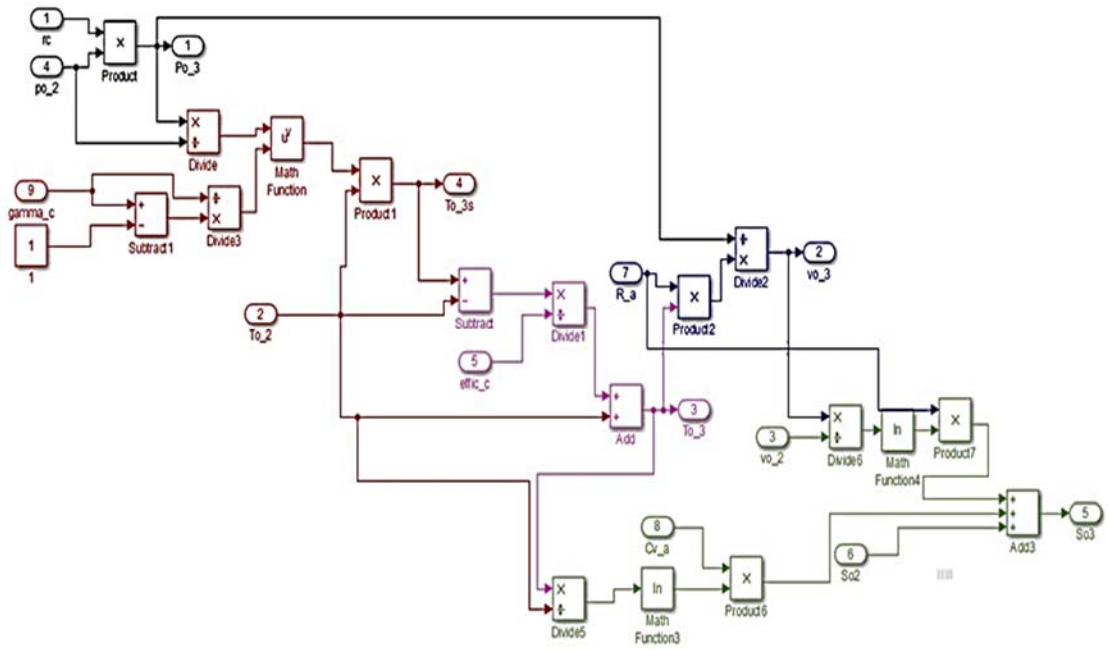

Figure 7: Compressor model.

Turbojet Engine Model

Figure (8) shows the complete turbojet engine model that comprises of all models of the components.

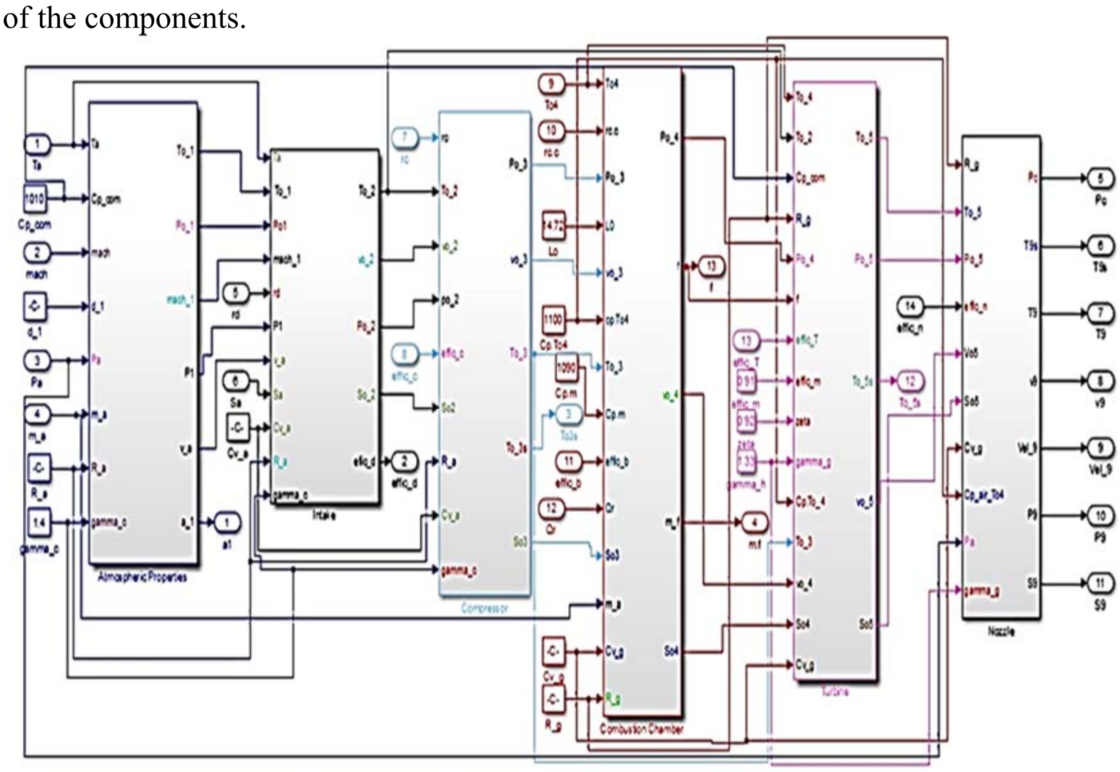

Figure 8: Simulink model of turbojet engine.

Performance Calculation

The engine performance parameters are modelled in Simulink as shown in Figure (9).

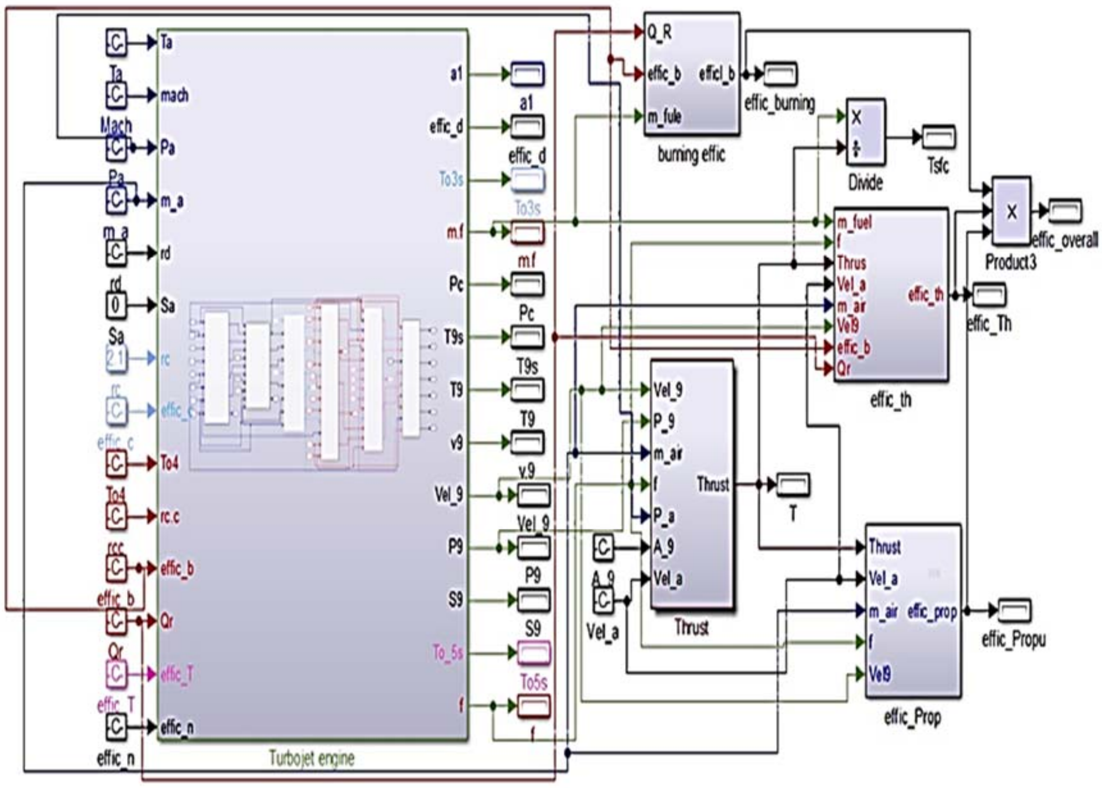

Figure 9: Performance calculation.

RESULTS AND ANALYSIS

Table (4) shows the maximum numerical values of some of the important outputs of simulated model and real engine test data versus different variables for comparison.

Table 4: Output Data

Outputs		Derived model	Real engine	Error (%)
τ_{max} (N)	f = 0.2	114.1	104	9.7
TSFC		0.001361	0.001524	10.5
τ_{max} (N)	$\dot{m} = 0.8$ kg/s	117.6	105	12
η_p		0.6133	0.591	3.8
η_{th}		0.0731	0.1185	38.3
η_o		0.04005	0.06759	40.7
τ_{max} (N)	$V_e = 300$ m/s	118.7	117.7	0.85
η_p		0.5686	0.5696	0.17
η_{th}		0.08517	0.1598	46.7
η_o		0.04512	0.0845	46.6

The comparison shows differences between the simulated and real results. The difference in thrust is about 12% and 9.7% versus the mass flow rate and the fuel to air ratio respectively, while the difference of thrust versus the exit velocity is reasonable, about 0.85%. The TSFC difference is about 10.5% from the real. In addition, the propulsive efficiency differences are reasonable with values of 3.8% and 0.17% for mass flow rate and exit velocity respectively. The high values of thermal efficiency differences of 38.3% and 46.7%, leads to high differences in the overall efficiency as 40.7% and 46.4%. These differences are due to the assumed efficiencies values of the different engine components since the real values are not available and the simplifications that made in deriving the mathematical model. Figure (10) shows the variation of engine's rpm versus time from startup and gradually increases until it reaches its maximum and then the engine shut down.

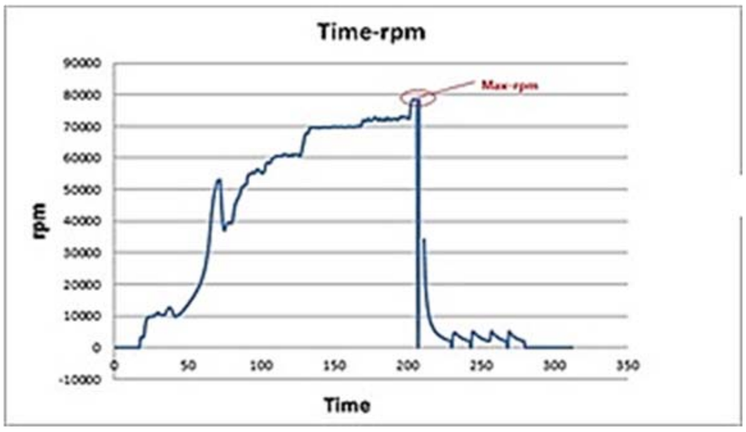

Figure 10: Relation between time and rpm.

Figure (11) shows the engine's T-s diagram. It is clear from the vure that the entropy increases with increasing the temperature, and at higher pressures, the temperature to entropy slope is larger. The change in temperature to change in entropy ratio for a process should be as high as possible to maximize the efficiency. It can be noted that the effects of compression efficiency can be seen as a change in entropy moving from Point (a to 3). The turbine efficiency causes a rise in entropy as the cycle moves from Point (4) to (5). Pressure loss in the burner can be seen, as points 3 and 4 are no longer on the same pressure curve. Nozzle efficiency in the form of excess pressure and other losses can be noticed as an increase in entropy from Points 5 to 9 shows the returning of the cycle to the ambient pressure, and the length of line between points (5) and (9) is directly related to the amount of work output by the cycle, which is converted to thrust force in the nozzle. The points described in this section coincide with the station numbering scheme used in Figure (2). Figure (12) shows that the thrust force is linearly increasing with increasing the exit velocity. The difference between the two curves is very small.

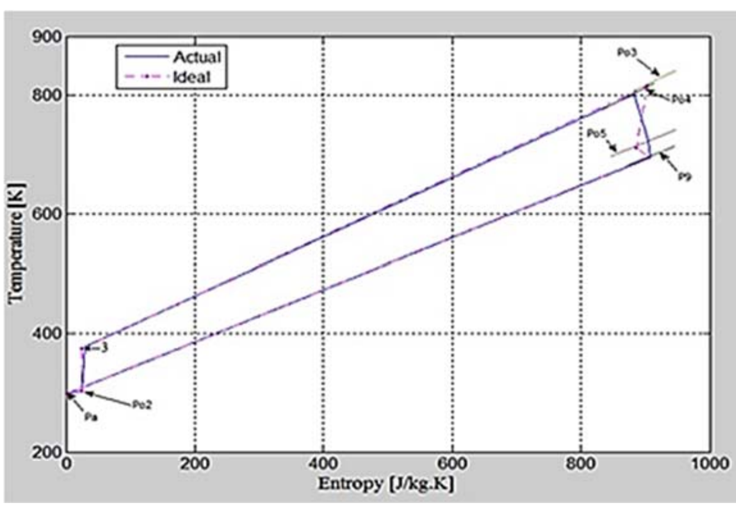

Figure 11: T-s diagram for Turbojet Engine.

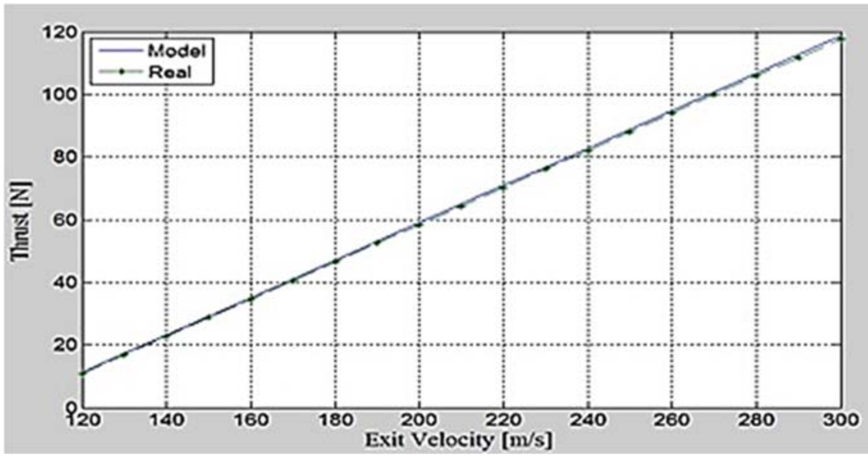

Figure 12: Relation between thrust and exit velocity

The thrust force increase is slow with the increase of fuel-to-air ratio and the difference between the two models is approximately constant because of low effect on the thrust, see Figure (13). While Figure (14) shows the large effect of the mass flow rate on increasing the thrust. The fuel to air ratio has a valuable effect on the specific fuel consumption (TSFC), Figure (15). The differences between the two models in these Figures (14 and 15) increases as the mass flow rate and fuel to air ratio increases respectively.

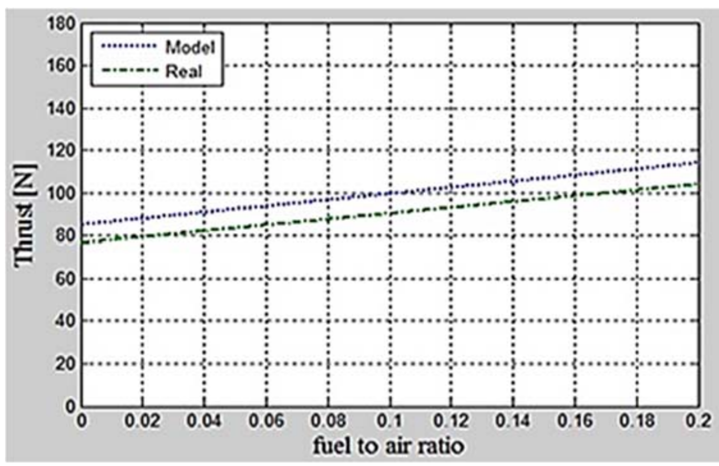

Figure 13: Thrust and fuel to air ratio.

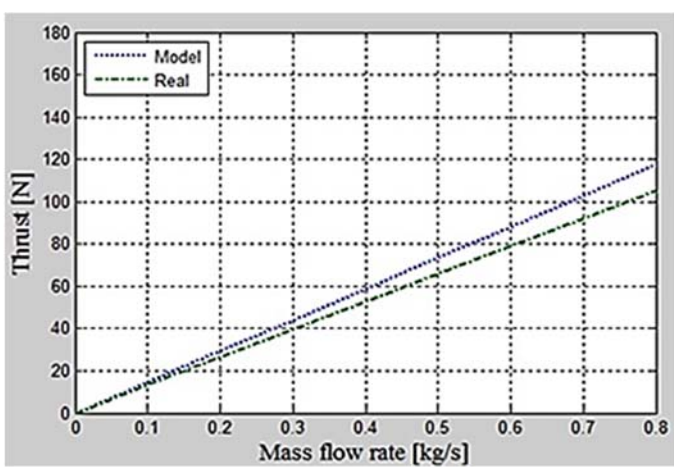

Figure 14: Thrust – air mass flow rate.

Figures (16) and (17) show very small increases in the thermal efficiency versus the increase in the exit velocity and mass flow rate respectively, which may be because of the approximated values of η_b and Q_r. Again, the differences between the two models increases with the exit velocity and mass flow rate respectively. The same happen in Figure (18) for the variation of the overall efficiency with the exit velocity because the overall efficiency is a function of the thermal efficiency.

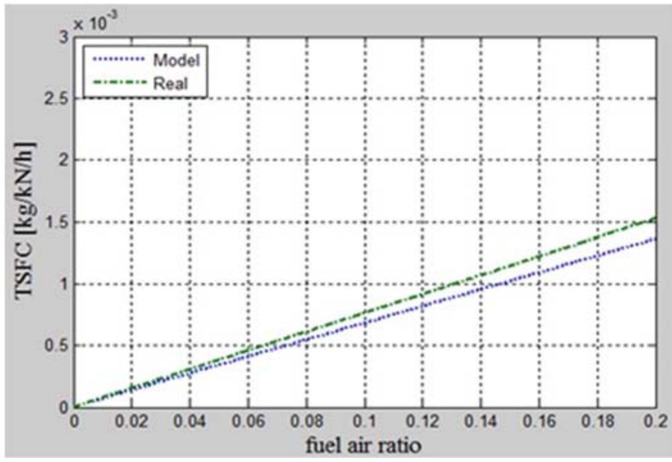

Figure 15: Relation between fuel/air ratio and TSFC.

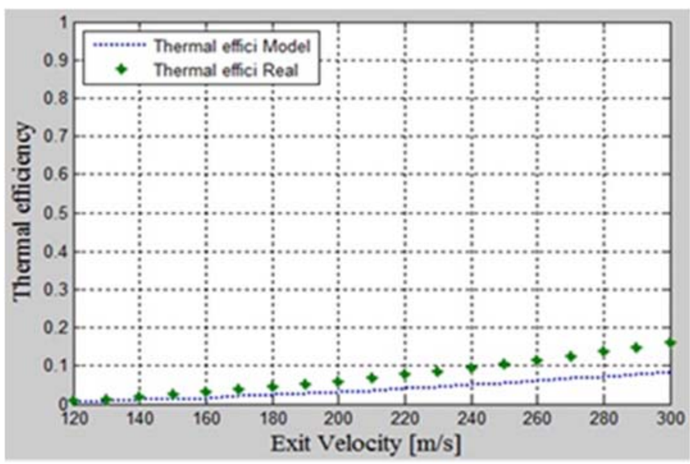

Figure 16: Thermal efficiency – exit velocity.

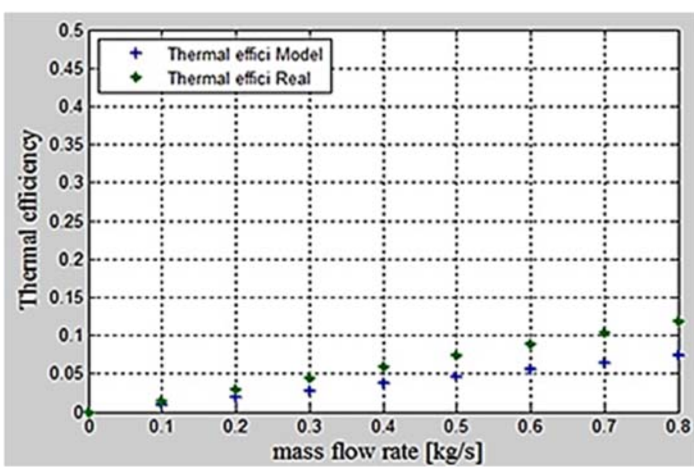

Figure 17: Thermal efficiency-mass flow rate.

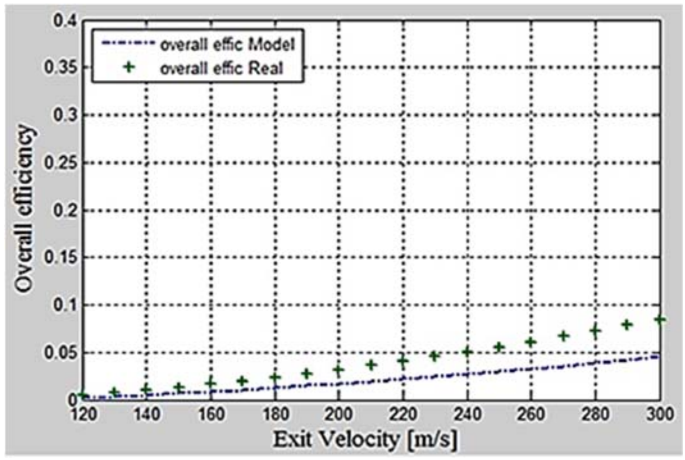

Figure 18: Overall efficiency with exit velocity.

The propulsive efficiency decreases with the increase of the exit velocity as in equation (5), this relation is plotted in Figure (19). Figure (20) shows that the air mass flow rate has not much significance on the propulsive efficiency, so, its changes can be negligible and considered constant. These differences are mainly due to the assumed efficiencies values of the different engine components; since the real values for the real engine are not available, the used ones were taken from a similar work [14].

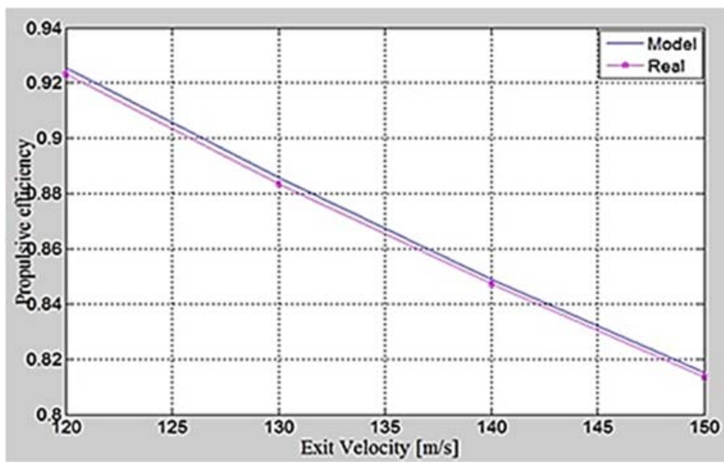

Figure 19: The effect of exit velocity on the propulsive efficiency.

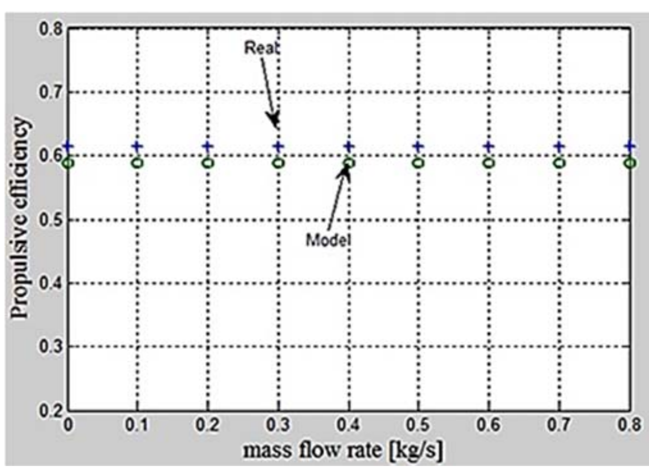

Figure 20: Relationship between mass flow rate and propulsive efficiency.

CONCLUSIONS

This work presented is derivation of a mathematical model for the CM14 laboratory model of a single spool turbojet engine by deriving the detailed equations for the different engine components. The derived model then simulated using MATLAB and Simulink to evaluate the engine performance by studying the engine performance parameters. The results from the derived model then compared with that from real engine tests, which show some differences in the performance parameters. These differences are due to the assumed efficiencies values of the different engine components since the real values are not available and the simplifications made in deriving the mathematical model. So, the derived model is considered reasonable and satisfied. Further studies include improving the values of the as summed efficiencies as well as using the derived mathematical model in calculating the engine performance parameters at different conditions and different operating points as well as in designing some of control methods for the engine.

LIST OF SYMBOLS

Symbol	Definition	Unit		Symbol	Definition	Unit
A	Area	[m^2]		c_v	Specific heat at constant volume	[J/kg·K]
f	Fuel-to-air ratio	—		r_d	Intake pressure recovery factor	—
M	Mach number	—		r_c	Compressor total pressure ratio	—
$\dot{m}_f$	Fuel mass flow rate	[kg/s]		$r_{c.c}$	Combustion chamber pressure loss	—
$\dot{m}_a$	Mass flow rate of air	[kg/s]		r_n	Nozzle pressure ratio	—
P	Pressure	[Pa]		γ	Specific heat ratio	—
P_a	Ambient static pressure	[Pa]		ρ	Fluid density	[kg/m^3]
R	Gas constant	[J/kg]		η_b	Burner efficiency	—
R_M	Universal gas constant	[J/kmol.K]		η_C	Compressor isentropic efficiency	—
Q_r	Fuel heating value	[kJ/kg]		η_d	Diffuser efficiency	—
S	Entropy	[J/kg.K]		η_m	Mechanical efficiency	—
T	Temperature	[k]		η_n	Isentropic efficiency of a nozzle	—
v	Specific volume	[m^3/kg]		η_P	Propulsive efficiency	—
V_a	Flight speed	[m/s]		η_t	Isentropic efficiency of turbine	—
TSFC	Thrust Specific Fuel Consumption	[kg/kN./h]		η_{th}	Engine Thermal efficiency	—
c_p	Specific heat at constant pressure	[J/kg·K]		τ	Thrust	[kN]

REFERENCES

[1] El-Sayed, A., “Aircraft Propulsion and Gas Turbine Engines”, Zagazig University, 2008.

[2] CM14: Axial Flow Turbine Engine, http://www.google.com/Gas Turbine engine.

[3] Zare, F., Dr. Veress, Á., and Beneda, K., “Simplified Mathematical Model for A Single Spool and No Bypass Jet Engine”, RTK Conference, BME, 2013.

[4] Ujam, A., Ifeacho, F. and Anakudo, G., “Modeling Performance Characteristics of a Turbojet Engine”, Department of Mechanical and production Engineering, Enugu State University of Science and Technology,

Enugu, Nigeria, Calabar, Nigeria. Published by European Centre for Research Training and Development UK, September 2013.

[5] Tudosie, A. N.,” Turbo-Jet Engine’s Rotation Speed Control System with Fuel Flow Rate Injection Controller. International Conference on Electromechanical and Power Systems”, University of Craiova, Faculty of Electrical Engineering, Avionics Department, October 4-6, 2007.

[6] Tudosie, A. N., “Mathematical Model of a Jet Engine Afterburning Fuel System”, Avionics Department, Faculty of Electrical Engineering University of Craiova 105-107 Decebal Blvd., Craiova, Dolj Romania, 15 May 2015.

[7] Tudosie, A. N., and SEPCU, C. L., “Single-Spool Jet Engine for Aircraft with Afterburning Systems”, University of Craiova, Faculty of Electrical Engineering, Avionics Department, Annals of the University of Craiova, Electrical Engineering series, No. 34, 2010, ISSN 1842-4805.

[8] Abeykoon, C., Modelling of a Turbojet Gas Turbine Engine, the University of Manchester, September 2015.

[9] Afiz1, I. A., Cunliffe1, R., Alukaidey, T., “Mathematical Modeling and Simulation of a Twin-Engine Aircraft Fuel System Using MATLAB-Simulink”, International Journal of Control Science and Engineering, 2018, 8(1), 1-12.

[10] Chachurski, R., Trzeciak, A., Jędrowiak, B., “Comparison of the results of mathematical modeling of a GTM 120 miniature turbine jet engine with the research results”, Combustion Engines, 2018, 173(2), 30-33.

[11] Singh, R., Maity, A., and Nataraj, P.S.V., “Modeling, Simulation and Validation of Mini SR-30 Gas Turbine Engine”, IFAC Papers Online, 51-1, 2018, 554-559.

[12] Velásquez-SanMartín, F., Insausti, X., Zárraga-Rodríguez, M., and Gutiérrez-Gutiérrez, J., "A Mathematical Model for the Analysis of Jet Engine Fuel Consumption during Aircraft Cruise" Energies 14, no. 12: 3649, June 2021.

[13] Farokhi, S. “Aircraft Propulsion”, Second Edition, the University of Kansas, USA, 2014.

[14] Rolls-Royce plc, "The Jet Engine”, Fifth edition, the Technical Publications Department, England, 1996.